Atmospheric impacts of chlorinated very short-lived substances over the recent past - Part 2: Impacts on ozone

Ewa M. Bednarz[1,2,3], Ryan Hossaini[1,4], Martyn P. Chipperfield[5,6]

1. Lancaster Environment Centre, Lancaster University, Lancaster, UK
2. Cooperative Institute for Research in Environmental Science (CIRES), University of Colorado Boulder, Boulder, CO, USA.
3. NOAA Chemical Sciences Laboratory (NOAA CSL), Boulder, CO, USA
4. Centre of Excellence in Environmental Data Science (CEEDS), Lancaster University, Lancaster UK.
5. School of Earth and Environment, University of Leeds, Leeds, UK
6. National Centre for Earth Observation (NCEO), University of Leeds, Leeds, UK

Correspondence to: Ewa M. Bednarz (ewa.bednarz@noaa.gov)

Abstract

Depletion of the stratospheric ozone layer remains an ongoing environmental issue, with increasing stratospheric chlorine from Very Short-Lived Substances (VSLS) recently emerging as a potential but uncertain threat to its future recovery. Here the impact of chlorinated VSLS on past ozone is quantified, for the first time. using the UM-UKCA chemistry-climate model. Model simulations show that between 2010-2019 Cl-VSLS reduced total column ozone by, on average, ~2-3 DU in the springtime high latitudes and by ~0.5-1 DU in the tropics, with up to 5-6 DU monthly and zonal mean Arctic ozone reductions simulated in the springs of 2011, 2014 and 2020. Cl-VSLS impacts during the recent cold Arctic winter of 2019/2020 are also quantified to have resulted in up to 6 % reduction of lower stratospheric ozone and ~6 DU ozone in total by the end of March. On the other hand, the simulations show that the inclusion of Cl-VSLS does not considerably modify the magnitude of the diagnosed recent ozone trends. We also estimate the ozone depletion potential of dichloromethane, the most abundant Cl-VSLS, at 0.0107. Our results thus illustrate a so-far modest but nonetheless non-negligible role of Cl-VSLS in contributing to stratospheric ozone budget over the recent past that if to continue could offset some of the gains achieved by the Montreal Protocol.

1. Introduction

Depletion of the stratospheric ozone layer remains an ongoing environmental issue, caused predominantly by long-lived ozone-depleting substances (ODSs) containing chlorine and bromine. Controls on the production of ODSs, such as chlorofluorocarbons, introduced by the Montreal Protocol and its amendments have successfully reduced the stratospheric loading of chlorine and bromine (e.g. Bernath and Fernando, 2018) and thus it is expected that ozone should return to pre-1980 levels in the middle to latter half of this century (WMO, 2022). However, in recent years it has been became evident that

so-called Very Short-Lived Substances (VSLS), with lifetimes in the near-surface atmosphere of less than ~6 months, also provide a significant source of stratospheric halogens (e.g. Fernandez et al., 2014; Wales et al., 2018; Keber et al., 2020). While brominated VSLS (e.g. $CHBr_3$) are typically of natural ocean origin, recent studies have raised concerns that unregulated

35   industrial emissions of chlorinated VSLS (Cl-VSLS) are offsetting some of the gains of the Montreal Protocol (e.g. Hossaini et al., 2019; Bednarz et al., 2022) and could thus delay future recovery of the ozone layer (Hossaini et al., 2017).

Dichloromethane (CH_2Cl_2) is a common solvent used in a wide variety of applications and is the most abundant atmospheric Cl-VSLS. Global CH_2Cl_2 emissions in 2020 were estimated at ~1.1 Tg/yr, a factor 2.5 increase from the year 2000 (WMO,

40   2022) that has been due predominately to growth in Asia (Claxton et al., 2020; An et al., 2021). The ozone depletion potential (ODP) of CH_2Cl_2 has been estimated to be ~0.01-0.02 (Claxton et al., 2019), though despite recent strong interest in this gas there has not been more estimates of this important policy metric. Other Cl-VSLS with significant industrial sources include chloroform ($CHCl_3$), Asian emissions of which have also grown substantially (Fang et al., 2019), 1,2-dichloroethane (CH_2ClCH_2Cl) and perchloroethylene (C_2Cl_4). In Part 1 of this study (Bednarz et al., 2022), we investigated the impacts of

45   these Cl-VSLS on the stratospheric chlorine budget using the Unified Model coupled to the United Kingdom Chemistry and Aerosol (UM-UKCA, Walters et al., 2019; Archibald et al., 2020) chemistry-climate model (CCM). We showed that the contribution from these Cl-VSLS to stratospheric chlorine had increased from 70 ppt Cl in 2000 to 130 ppt Cl in 2019, i.e. almost doubling over the first two decades of the 21st century.

50   Evidence of ozone layer recovery is apparent in the polar stratosphere from observations and models (e.g. Solomon et al., 2016; Kuttippurath et al., 2018; WMO, 2022). However, a persistent downward trend in extra-polar lower stratospheric ozone has been reported from datasets based on satellite observations (e.g. Ball et al., 2018; 2019). In this region, ozone is strongly affected by dynamical variability (Chipperfield et al., 2018) and the downward ozone trend is likely associated with large-scale changes to atmospheric circulation (Wargan et al., 2018; Orbe et al., 2020). Although it has established that VSLS can

55   impact ozone in the lower stratosphere (e.g. Hossaini et al., 2015), the effect of Cl-VSLS on the above ozone trend has been estimated to be small (Chipperfield et al., 2018). However, this issue has yet to be examined using a global model containing a coupled troposphere-stratosphere chemistry scheme. Moreover, the effects of Cl-VSLS on ozone more broadly, including their contribution to some of the strong Arctic ozone depletions observed in the recent past (e.g. Feng et al., 2021), is unknown.

60   The impacts of Cl-VSLS on stratospheric ozone and ozone trends are thus the focus of this Part 2 of our study. Part 1 (Bednarz et al., 2022a) highlighted important differences in the stratospheric Cl-VSLS levels simulated in free-running and nudged UM-UKCA model versions (including differences brought about by the choice of reanalysis used for nudging). Hence ozone impacts are investigated here using three sets of transient simulations over the recent past (1990 onwards), both with and without Cl-VSLS included. These are (1) VSLS and BASE that have free-running meteorology, (2) $VSLS_{SD-5}$ and $BASE_{SD-5}$

65   that are nudged to the ECMWF ERA5 reanalysis, and (3) $VSLS_{SD-I}$ and $BASE_{SD-I}$ that are nudged to the ECMWF ERA-Interim

reanalysis. The simulations are described in more detail in the Methods section. We quantify the impacts of Cl-VSLS on ozone over the beginning of the 21st century (Section 2), including the contribution of Cl-VSLS to the elevated ClO and reduced ozone observed during the recent very cold Arctic winter of 2019/2020 (Section 3). We also discuss the contribution of Cl-VSLS to the recent ozone trends (Section 4), as well as use additional UM-UKCA simulations to calculate ODP of CH$_2$Cl$_2$
70   (Section 5). Summary and conclusions are given in Section 6.

2. Impacts on ozone in the second decade of 21st century

Figure 1 shows the difference in total column ozone between the integrations with and without Cl-VSLS as a function of latitude and time (from January 2010 onwards), for the simulations nudged to either ERA5 (Fig.1a) or ERA-Interim (Fig. 1b) reanalysis. Given the significant dynamical variability characterising ozone levels on year-to-year timescales, we focus here
75   on the results from the nudged runs only.

The integrations nudged to ERA5 show springtime ozone losses of up to ~3-5 DU in both the Northern Hemisphere (NH) and Southern Hemisphere (SH) high latitudes. For the Arctic, the largest springtime ozone losses of up to 5-6 DU (monthly and zonal mean) were simulated in the years 2011, 2014 and 2020, i.e. under the formation of a strong, cold and relatively long-
80   lasting NH polar vortex (Manney et al., 2011; Sinnhuber et al., 2011). Yet, ozone reductions of 2-3 DU in spring (Fig. 1c) are found on average each year even for warm winters. Interestingly, slightly smaller total column ozone changes are diagnosed from the simulations nudged to ERA-Interim (Fig.1b and Fig. 1c). This could be due to the higher levels of chlorine from Cl-VSLS found in the stratosphere in the form of Cl-VSLS source gases (Bednarz et al., 2022a). Furthermore, no significant Cl-VSLS-induced Arctic ozone loss can be diagnosed from the model ERA-Interim nudged monthly and zonal mean data for the
85   spring 2011; this might be related to the small size of the polar vortex in that year and thus difficulties in reproducing its dynamical properties in a nudged model set up. These results thus suggest that the choice of reanalysis chosen for nudging can also be important in some years for the diagnosed ozone impacts from Cl-VSLS. In the tropics, Cl-VSLS reduce column ozone by up to ~1 DU over the final few years of the simulations nudged to ERA5; whilst small in absolute terms, these can play a comparatively larger role for surface UV due to climatological ozone being much lower there than at higher latitudes, and the
90   smaller daytime solar zenith angles.

Vertically resolved ozone changes show that the impacts of Cl-VSLS are largest in the lower stratosphere (Fig. 2). The inclusion of Cl-VSLS results, on average, in a ~0.5-1 % yearly mean ozone reduction in the tropical lower stratosphere over the final decade of the integration (2010-2019; Fig. 2a). Larger ozone reductions occur in the SH high latitudes during spring,
95   up to ~3.5 % (Fig. 2b), with a further 1-1.5 % average reduction over the Arctic in March (Fig. 2c). Overall qualitatively and quantitatively similar O$_3$ responses are found if only the last 3 years of the integrations (2017-2019) are considered (Fig. S1), i.e. when the contribution of Cl-VSLS to the stratospheric chlorine budget is largest.

3 Impacts during Arctic winter 2019/2020

The recent decade has seen a number of strong Arctic ozone depletion episodes reported from the observational record (WMO,
100   2018). Amongst these was the Arctic winter of 2019/2020, where the formation of strong, cold and relatively undisturbed polar
vortex led to one of the largest Arctic ozone depletions observed in the recent past (e.g. Manney et al., 2020; Feng et al., 2021;
Wohltmann et al., 2020; Lawrence et al., 2020; Inness et al., 2020).

Consistent with the observations, significantly elevated ClO concentrations (up to 800 ppt ClO at 50 hPa on 1 March 2020,
105   Fig. 3c) were simulated in the Arctic in spring in the UM-UKCA simulation nudged to the ERA5 reanalysis (VSLS$_{SD5}$).
Comparison with the BASE$_{SD5}$ run that did not include Cl-VSLS shows that up to ~25 ppt of the elevated ClO concentrations
were of Cl-VSLSs origin (Fig. 3f). Increased chlorine- and bromine-catalysed ozone depletion along with reduced transport of
higher ozone levels from the mid-latitudes and/or higher altitudes resulted in very low ozone levels simulated in the Arctic at
the end of March. Ozone levels of less than 1 ppb at 50 hPa were simulated in VSLS$_{SD5}$ on 31 March (Fig. 3b), corresponding
110   to the minimum in the total column values of less than 240 DU at the same time (Fig. 3a). We find that Cl-VSLS on their own
reduced ozone by up ~6 % at 50 hPa (Fig. 3e) and by up to ~6 DU in total by the end of March (Fig. 3d). Only slightly higher
total column ozone losses of up 7 DU are simulated in early April (Fig. S2)

In comparison, the impact of curbing emissions of long-lived ODSs achieved by the Montreal Protocol was estimated to reduce
115   the magnitude of the Arctic ozone depletion in that spring by up to ~35 DU in mid-March compared to peak halogen levels in
early 2000 (Feng et al., 2021). This illustrates that Cl-VSLS emissions have played a modest but nonetheless important
contribution to one of the largest stratospheric ozone depletion episodes observed in the Arctic, and by doing so acted to
significantly offset some of the environmental gains achieved by the Montreal Protocol to date.

4. Contribution to the recent ozone trends

120   Despite ongoing recovery of stratospheric ozone, observational evidence suggests existence of negative ozone trends over the
recent past in the tropical and mid- latitude lower stratosphere, and the causes behind these are still not fully understood (Ball
et al., 2018, 2020). Both vn2.6 and vn2.7 of the SWOOSH merged satellite ozone product (Davis et al., 2016) show negative
ozone trends over 2000-2019 throughout the tropical lower stratosphere and in the mid-latitudes of both hemispheres at the
altitudes of ~150 hPa and ~50 hPa (Fig. 4a-b).
125

All UM-UKCA simulations used here show negative ozone trends over the same period (2000-2019) in the tropical lower
stratosphere (Fig. 4c-h), in line with the GHG-induced acceleration of upwelling in the tropical troposphere (not shown). All
ERA5 and ERA-Interim nudged simulations also reproduce qualitatively the observed negative trends in the SH mid-latitudes,
with statistically significant trends that maximise at two altitudes in the lower stratosphere. This is not the case for the free-

130 running simulations, which show positive trends in the SH instead and a suggestion of small negative (but statistically not significant) ozone trends in the NH mid-latitudes. This highlights that the UM-UKCA model is capable of reproducing some of the negative lower stratospheric ozone trends seen from the observations, but the exact structure of the response depends on the choice of model-set up, highlighting the importance of the model dynamical fields in reproducing the observed response.

135 Regarding the role of Cl-VSLS, we find that the magnitudes of the lower stratospheric trends are very similar between the pairs of runs with and without Cl-VSLS. The derived trends are only slightly more negative or less positive with the inclusion of Cl-VSLS (Figure S3). This suggest that the increasing Cl-VSLS emissions over the recent past are unlikely to be the main contributor to the negative lower stratospheric ozone trends reported from the observations. Our results are thus in agreement with the conclusion of Chipperfield et al. (2018).

140 **5. Ozone Depleting Potential of CH$_2$Cl$_2$**

In the final part of this study we quantify the ODP and stratospheric ODP of CH$_2$Cl$_2$ using the time-slice simulations described in the Methods section. The responses of modelled annual mean ozone to CFC11 and CH$_2$Cl$_2$ perturbations are shown in Fig. S4, and the global mean changes are summarised in Table 1. From these data, we calculate the CH$_2$Cl$_2$ ODP of 0.0107 (with the associated ±2 standard error confidence interval of 0.0064-0.0175, Table 1). This result constitutes, to our knowledge, only

145 the second estimate of CH$_2$Cl$_2$ ODP in literature, and falls within the range of 0.0097-0.0208 reported in Claxton et al. (2019). The calculated stratospheric ODP of 0.0102 (confidence interval of 0.0062-0.0163) is similar to the whole atmosphere ODP metric, implying that CH$_2$Cl$_2$ has a relatively small effect on ozone below the tropopause in UM-UKCA.

6. Summary and conclusions

By controlling the production and use of long-lived ozone-depleting substances, the Montreal Protocol has been immensely

150 successful in reducing the abundance of atmospheric halogens (chlorine and bromine). In consequence, Earth's ozone layer is on a slow pathway to recovery. However, this landmark agreement faces new challenges, including the rapid growth of ozone-depleting chlorinated very short-lived substances. In this study, we have quantified for the first time the time-varying impact of uncontrolled Cl-VSLS emissions on stratospheric ozone, using the state-of-the-art UM-UKCA chemistry-climate model.

155 Between 2010-2019 Cl-VSLS reduced ozone, on average, by ~2-3 DU in the springtime high latitudes and by ~0.5-1 DU in the tropics. For the Arctic, we find considerable ozone reductions of up to 5-6 DU (monthly and zonal mean) in the springs of 2011, 2014 and 2020, although ozone reductions of 2-3 DU in spring are found for other years when no strong and long-lived polar vortex was formed. We note some dependence of the exact results on the choice of the reanalysis used for nudging. We also quantified the Cl-VSLSs impacts during the recent Arctic winter of 2019/2020, where the formation of strong and cold

160   polar vortex led to one of the largest Arctic stratospheric ozone depletion episodes in the observational record. In this case, Cl-VSLSs resulted in up to 6 % reduction of lower stratospheric ozone by the end of March, contributing to ~6 DU ozone depletion to the overall Arctic ozone anomaly.

Regarding recent ozone trends, the study shows that the inclusion of Cl-VSLS does not considerably modify the magnitude of
165   the diagnosed trends. However, we show the UM-UKCA model is capable of reproducing the negative lower stratospheric ozone trends reported from the satellite observations in the tropics and mid-latitudes, but the exact structure of the response depends on the choice of model-set up, indicating the importance of the model dynamical fields in reproducing the observed response.

170   Our results illustrate a so-far modest but nonetheless important role of Cl-VSLS in contributing to the stratospheric ozone budget over the recent past. If the growth in Cl-VSLS emissions inferred in the last decade (Feng et al., 2018; Fang et al., 2019, Claxton et al., 2020) continues into the future, these gases could exert larger influence on future stratospheric ozone levels and, thus, continue to offset some of the gains achieved by the Montreal Protocol and delay the recovery of the ozone layer.

175   **Acknowledgements**

The authors acknowledge support from the UK Natural Environment Research Council (NERC) SISLAC project (NE/R001782/1), NERC Independent Research Fellowship (NE/N014375/1), and NERC ISHOC project (NE/R004927/1). EMB also acknowledges support from the NOAA cooperative agreement NA22OAR4320151.
The simulations were carried out using MONSooN2, a collaborative high performance computing facility funded by the Met
180   Office and the Natural Environment Research Council, and using the ARCHER UK National Supercomputing Service.

Conflicting interests

The authors declare they have no conflict of interests.

Methods

1. Transient 1990-2019 UM-UKCA simulations

We use vn11.0 of the UM-UKCA CCM (Walters et al., 2019; Archibald et al., 2020), run in atmospheric-only mode with prescribed observed sea-surface temperatures and sea-ice. The chemistry scheme used is the recently developed Double Extended Stratospheric-Tropospheric (DEST vn1.0; Bednarz et al., 2022b) scheme that includes comprehensive stratospheric halogen chemistry. The simulations analysed here are described fully in Bednarz et al. (2022a). Briefly, they consist of 3 pairs – with and without Cl-VSLS - of transient 1990-2019 (or 1990-2020) experiments. Simulations with Cl-VSLS used imposed time- and latitudinally- varying lower boundary conditions (LBCs), derived using surface Cl-VSLS measurements from NOAA and AGAGE stations. The first pair of runs, termed VSLS (i.e. with Cl-VSLS) and BASE (i.e. no Cl-VSLS), used a free-running meteorology, with 3 ensemble members each to reduce the contribution of natural variability. The second pair, $VSLS_{SD5}$ and $BASE_{SD5}$, used meteorology nudged to the ERA5 reanalysis (Hersbach et al., 2020). The third pair, $VSLS_{SDI}$ and $BASE_{SDI}$, used meteorology nudged to the ERA-Interim reanalysis (Dee et al., 2011).

2. Time-slice UM-UKCA simulations

In addition to the transient simulations discussed above, we also ed a set of free-running 'time-slice' simulations under perpetual year 2015 conditions in order to calculate the ozone depletion potential (ODP) of CH_2Cl_2. In each case, the climatological sea-surface temperatures and sea-ice fields were the mean over the period 2011-2019 inclusive. Lower boundary conditions for ODSs and other long-lived gases for the year 2015 were taken from the SSP2-4.5 scenario, whilst the emissions of other chemical tracers corresponded to the averages over 2015-2016 conditions. The meteorology in these runs is free running. The simulations include: a base run; a simulation with an additional 100 ppt of CFC-11 at the surface relative to the base run; and a simulation with a 3 Tg/yr global CH_2Cl_2 source. For the latter, emissions were assumed to be evenly distributed over North America, Europe, and South-East Asia (Fig. S5). All simulations were run to steady-state, and then for additional 50 years that are used in the analysis.

3. Calculation of CH_2Cl_2 ozone depletion potential

The rate of CFC-11 emission corresponding to the 100 ppt surface increase is calculated at steady state, when the global emission of CFC11 equates to its global loss (via photolysis and the reactions with $O(^1D)$ and OH). This is calculated to be 0.0350 Tg/yr, in good agreement with estimates reported in previous ODP studies (e.g. Wuebbles et al., 2011). The ODP of CH_2Cl_2 can then be calculated following Eq. (1), where ΔTCO3 denotes the global annual mean total column ozone change due to a unit emission of either CH_2Cl_2 or CFC-11:

$$ODP(CH_2Cl_2) = \Delta TCO3(CH_2Cl_2) \ / \ \Delta TCO3(CFC\text{-}11) \qquad\qquad (Eq. 1)$$

For VSLS that have a non-negligible impact on tropospheric ozone, 'stratospheric ODP' may provide a more informative metric where the goal is to evaluate the effect of a substance on the ozone layer (Zhang et al., 2020). In that case, stratospheric ODP is calculated analogously using Eq. (2), where $\Delta SCO3$ denotes the corresponding annual mean stratospheric column ozone change (here approximated by not included the airmasses at or below the tropopause):

220

Stratospheric ODP(CH_2Cl_2) = $\Delta SCO3(CH_2Cl_2)$ / $\Delta SCO3$(CFC-11)   (Eq. 2)

4. Calculation of ozone trends

In Section 4 we discuss linear trends in de-seasonalised ozone values from December 1999 to August 2019 for the ensemble
225   mean free-running integrations as well as for each of the nudged runs. Following the procedure in Bednarz et al. (2022a), in each case zonal and monthly mean O_3 data are first interpolated onto a 10°-latitude grid and seasonally averaged (DJF, MAM, JJA and SON). The resulting seasonal mean time series are then de-seasonalised (i.e. long-term mean for each season was removed), and a simple linear trend is calculated. The same procedure is also performed for calculating trends in the observed ozone values as given by the vn2.6 and vn2.7 of the SWOOSH merged satellite ozone dataset (Davis et al., 2016).

230

References

An, M., Western, L.M., Say, D. L. Chen, T. Claxton, A.L. Ganesan, R. Hossaini, P.B. Krummel, A.J. Manning, J. Mühle, S. O'Doherty, R.G. Prinn, R.F. Weiss, D. Young, J. Hu, B. Yao, M. Rigby: Rapid increase in dichloromethane emissions from China inferred through atmospheric observations. Nat Commun 12, 7279, 2021.

235

Archibald, A. T., O'Connor, F. M., Abraham, N. L., Archer-Nicholls, S., Chipperfield, M. P., Dalvi, M., Folberth, G. A., Dennison, F., Dhomse, S. S., Griffiths, P. T., Hardacre, C., Hewitt, A. J., Hill, R. S., Johnson, C. E., Keeble, J., Köhler, M. O., Morgenstern, O., Mulcahy, J. P., Ordóñez, C., Pope, R. J., Rumbold, S. T., Russo, M. R., Savage, N. H., Sellar, A., Stringer, M., Turnock, S. T., Wild, O., and Zeng, G.: Description and evaluation of the UKCA stratosphere–troposphere chemistry scheme (StratTrop vn 1.0) implemented in UKESM1, Geosci. Model Dev., 13, 1223–1266, https://doi.org/10.5194/gmd-13-1223-2020, 2020.

240

Ball, W. T., Alsing, J., Mortlock, D. J., Staehelin, J., Haigh, J. D., Peter, T., Tummon, F., Stübi, R., Stenke, A., Anderson, J., Bourassa, A., Davis, S. M., Degenstein, D., Frith, S., Froidevaux, L., Roth, C., Sofieva, V., Wang, R., Wild, J., Yu, P., Ziemke, J. R., and Rozanov, E. V.: Evidence for a continuous decline in lower stratospheric ozone offsetting ozone layer recovery, Atmos. Chem. Phys., 18, 1379–1394, https://doi.org/10.5194/acp-18-1379-2018, 2018.

245

Ball, W. T., Alsing, J., Staehelin, J., Davis, S. M., Froidevaux, L., and Peter, T.: Stratospheric ozone trends for 1985–2018: sensitivity to recent large variability, Atmos. Chem. Phys., 19, 12731–12748, https://doi.org/10.5194/acp-19-12731-2019, 2019.

250

Ball, W. T., Chiodo, G., Abalos, M., Alsing, J., and Stenke, A.: Inconsistencies between chemistry–climate models and observed lower stratospheric ozone trends since 1998, Atmos. Chem. Phys., 20, 9737–9752, https://doi.org/10.5194/acp-20-9737-2020, 2020.

255

Bednarz, E. M., Hossaini, R., Chipperfield, M. P., Abraham, N. L., and Braesicke, P.: Atmospheric impacts of chlorinated very short-lived substances over the recent past – Part 1: Stratospheric chlorine budget and the role of transport, Atmos. Chem. Phys., 22, 10657–10676, https://doi.org/10.5194/acp-22-10657-2022, 2022a.

Bednarz, E. M., Hossaini, R., Abraham, L., and Chipperfield, M. P.: Description and evaluation of the new UM-UKCA (vn11.0) Double Extended Stratospheric-Troposphere (DEST vn1.0) scheme for comprehensive modelling of halogen chemistry in the stratosphere, Geosci. Model Dev. Discuss. [preprint], https://doi.org/10.5194/gmd-2022-215, in review, 2022b.

260

Bernath, P. and Fernando, A. M.: Trends in stratospheric HCl from the ACE satellite mission, J. Quant. Spectrosc. Ra., 217,
265 126–129, https://doi.org/10.1016/j.jqsrt.2018.05.027, 2018.

Claxton, T., Hossaini, R., Wilson, C., Montzka, S. A., Chipperfield, M. P., Wild, O., Bednarz, E. M., Carpenter, L. J., Andrews,
S. J., Hackenberg, S. C., Mühle, J., Oram, D., Park, S., Park, M.-K., Atlas, E., Navarro, M., Schauffler, S., Sherry, D., Vollmer,
M., Schuck, T., Engel, A., Krummel, P. B., Maione, M., Arduini, J., Saito, T., Yokouchi, Y., O'Doherty, S., Young, D., and
270 Lunder, C.: A synthesis inversion to constrain global emissions of two very short lived chlorocarbons: dichloromethane, and
perchloroethylene, J. Geophys. Res.-Atmos., 125, e2019JD031818, https://doi.org/10.1029/2019JD031818, 2020.

Claxton, T., Hossaini, R., Wild, O., Chipperfield, M. P., & Wilson, C.: On the regional and seasonal ozone depletion potential
of chlorinated very short-lived substances. Geophysical Research Letters, 46, 5489– 5498.
275 https://doi.org/10.1029/2018GL081455, 2019.

Chipperfield, M. P., Dhomse, S., Hossaini, R., Feng, W., Santee, M. L., Weber, M., Burrows, J.P., Wild, J.D., Loyola, D.,
Coldewey-Egbers, M.: On the cause of recent variations in lower stratospheric ozone. Geophysical Research Letters, 45,
5718– 5726. https://doi.org/10.1029/2018GL078071, 2018.
280
Davis, S. M., Rosenlof, K. H., Hassler, B., Hurst, D. F., Read, W. G., Vömel, H., Selkirk, H., Fujiwara, M., and Damadeo, R.:
The Stratospheric Water and Ozone Satellite Homogenized (SWOOSH) database: A long-term database for climate studies,
Earth System Science Data, doi:10.5194/essd-8-461-2016, 2016.

285 Dee, D. P., Uppala, S. M., Simmons, A. J., Berrisford, P., Poli, P., Kobayashi, S., Andrae, U., Balmaseda, M. A., Balsamo, G.,
Bauer, P., Bechtold, P., Beljaars, A. C. M., van de Berg, I., Biblot, J., Bormann, N., Delsol, C., Dragani, R., Fuentes, M., Greer,
A. J., Haimberger, L., Healy, S. B., Hersbach, H., Holm, E. V., Isaksen, L., Kallberg, P., Kohler, M., Matricardi, M., McNally,
A. P., Mong-Sanz, B. M., Morcette, J.-J., Park, B.-K., Peubey, C., de Rosnay, P., Tavolato, C., Thepaut, J. N., and Vitart, F.:
The ERA-Interim reanalysis: Configuration and performance of the data assimilation system, Q. J. Roy. Meteor. Soc., 137,
290 553–597, https://doi.org/10.1002/qj.828, 2011 (data available at: https://www.ecmwf.int/en/forecasts/datasets/reanalysis-
datasets/era-interim, last access: 18 July 2022).

Fang, X., Park, S., Saito, T., Tunnicliffe, R., Ganesan, A. L., Rigby, M., Li, S., Yokouchi, Y., Fraser, P. J., Harth, C. M.,
Krummel, P. B., Mühle, J., O'Doherty, S., Salameh, P. K., Simmonds, P. G., Weiss, R. F., Young, D., Lunt, M. F., Manning,
295 A. J., Gressent, A., and Prinn, R. G.: Rapid increase in ozone-depleting chloroform emissions from China, Nat. Geosci., 12,
89–93, 2019.

Feng, Y., Bie, P., Wang, Z., Wang, L., and Zhang, J.: Bottom-up anthropogenic dichloromethane emission estimates from China for the period 2005–2016 and predictions of future emissions, Atmos. Environ., 186, 241–247, https://doi.org/10.1016/j.atmosenv.2018.05.039, 2018.

Feng, W., S.S. Dhomse, C. Arosio, M. Weber, J.P. Burrows, M.L. Santee, and M.P. Chipperfield, Arctic ozone depletion in 2019/20: Roles of chemistry, dynamics and the Montreal Protocol, Geophys. Res. Lett., 48 (4), e2020GL091911, doi:10.1029/2020GL091911, 2021.

Fernandez, R. P., Salawitch, R. J., Kinnison, D. E., Lamarque, J.-F., and Saiz-Lopez, A.: Bromine partitioning in the tropical tropopause layer: implications for stratospheric injection, Atmos. Chem. Phys., 14, 13391–13410, https://doi.org/10.5194/acp-14-13391-2014, 2014.

Hersbach, H., Bell, B., Berrisford, P., Hirahara, S., Horányi, A., Muñoz-Sabater, J., Nicolas, J., Peubey, C., Radu, R., Schepers, D., Simmons, A., Soci, C., Abdalla, S., Abellan, X., Balsamo, G., Bechtold, P., Biavati, G., Bidlot, J., Bonavita, M., De Chiara, G., Dahlgren, P., Dee, D., Diamantakis, M., Dragani, R., Flemming, J., Forbes, R., Fuentes, M., Geer, A., Haimberger, L., Healy, S., Hogan, R. J., Hólm, E., Janisková, M., Keeley, S., Laloyaux, P., Lopez, P., Lupu, C., Radnoti, G., de Rosnay, P., Rozum, I., Vamborg, F., Villaume, S., and Thépaut, J.-N.: The ERA5 global reanalysis, Q. J. Roy. Meteor. Soc., 146, 1999–2049, https://doi.org/10.1002/qj.3803, 2020 (data available at: https://www.ecmwf.int/en/forecasts/datasets/reanalysis-datasets/era5, last access: 12 August 2022).

Hossaini, R., Atlas, E., Dhomse, S. S., Chipperfield, M. P., Bernath, P. F., Fernando, A. M., Mühle, J., Leeson, A. A., Montzka, S. A., Feng, W., Harrison, J. J., Krummel, P., Vollmer, M. K., Reimann, S., O'Doherty, S., Young, D., Maione, M., Arduini, J., and Lunder, C. R.: Recent trends in stratospheric chlorine from very short-lived substances, J. Geophys. Res.-Atmos., 124, 2318–2335, https://doi.org/10.1029/2018JD029400, 2019.

Hossaini, R., Chipperfield, M. P., Montzka, S. A., Leeson, A. A., Dhomse, S., & Pyle, J. A.: The increasing threat to stratospheric ozone from dichloromethane. Nature Communications, 8, 15962. https://doi.org/10.1038/ncomms15962, 2017.

Inness, A., S. Chabrillat, J. Flemming, V. Huijnen, B. Langenrock, J. Nicolas, I. Polichtchouk, and M. Razinger, Exceptionally low Arctic stratospheric ozone in spring 2020 as seen in the CAMS reanalysis, J. Geophys. Res. Atmos., 125 (23), e2020JD033563, doi:10.1029/2020JD033563, 2020.

Keber, T., Bönisch, H., Hartick, C., Hauck, M., Lefrancois, F., Obersteiner, F., Ringsdorf, A., Schohl, N., Schuck, T., Hossaini, R., Graf, P., Jöckel, P., and Engel, A.: Bromine from short-lived source gases in the extratropical northern hemispheric upper

troposphere and lower stratosphere (UTLS), Atmos. Chem. Phys., 20, 4105–4132, https://doi.org/10.5194/acp-20-4105-2020, 2020.

Kuttippurath, J., P. Kumar, P.J. Nair, and P.C. Pandey, Emergence of ozone recovery evidenced by reduction in the occurrence

335   of Antarctic ozone loss saturation, npj Clim. Atmos. Sci., 1 (1), 42, doi:10.1038/s41612-018-0052-6, 2018.

Lawrence, Z.D., J. Perlwitz, A.H. Butler, G.L. Manney, P.A. Newman, S.H. Lee, and E.R. Nash, The remarkably strong Arctic stratospheric polar vortex of winter 2020: Links to record-breaking Arctic Oscillation and ozone loss, J. Geophys. Res., 125 (22), e2020JD033271, doi:10.1029/2020JD033271, 2020

340   Manney, G.L., N.J. Livesey, M.L. Santee, L. Froidevaux, A. Lambert, Z.D. Lawrence, L.F. Millán, J.L. Neu, W.G. Read, M.J. Schwartz, and R.A. Fuller, Record-low Arctic stratospheric ozone in 2020: MLS observations of chemical processes and comparisons with previous extreme winters, Geophys. Res. Lett., 47 (16), e2020GL089063, doi:10.1029/2020GL089063, 2020.

345   Manney, G. L., Santee, M. L., Rex, M., Livesey, N. J., Pitts, M. C., Veefkind, P., Nash, E. R., Wohltmann, I., Lehmann, R., Froidevaux, L., Poole, L. R., Schoeberl, M. R., Haffner, D. P., Davies, J., Dorokhov, V., Gernandt, H., Johnson, B., Kivi, R., Kyro, E., Larsen, N., Levelt, P. F., Makshtas, A., McElroy, C. T., Nakajima, H., Parrondo, M. C., Tarasick, D. W., von der Gathen, P., Walker, K. A., and Zinoviev, N. S.: Unprecedented Arctic ozone loss in 2011, Nature, 478, 469-U465, 10.1038/nature10556, 2011.

350

Orbe, C., Wargan, K., Pawson, S., & Oman, L. D:. Mechanisms linked to recent ozone decreases in the Northern Hemisphere lower   stratosphere.   Journal   of   Geophysical   Research: Atmospheres,   125,   e2019JD031631. https://doi.org/10.1029/2019JD031631, 2020.

355   Sinnhuber, B.-M., Stiller, G., Ruhnke, R., von Clarmann, T., Kellmann, S., and Aschmann, J.: Arctic winter 2010/2011 at the brink of an ozone hole, Geophys. Res. Lett., 38, L24814, doi:10.1029/2011GL049784., 2011

Solomon, S., D.J. Ivy, D. Kinnison, M.J. Mills, R.R. Neely, A. Schmidt, Emergence of healing in the Antarctic ozone layer, Science, 353, pp. 269-274, 2016.

360

World Meteorological Organization (WMO), Scientific Assessment of Ozone Depletion: 2022, GAW Report No. 278, 509 pp., WMO, Geneva, 2022.

Wales, P. A., Salawitch, R. J., Nicely, J. M., Anderson, D. C., Canty, T. P., Baidar, S., Dix, B., Koenig, T. K., Volkamer, R.,
365   Chen, D., Huey, L. G., Tanner, D. J., Cuevas, C. A., Fernandez, R. P., Kinnison, D. E., Lamarque, J.-F., Saiz-Lopez, A., Atlas,
E. L., Hall, S. R., Navarro, M. A., Pan, L. L., Schauffler, S. M., Stell, M., Tilmes, S., Ullmann, K., Weinheimer, A. J., Akiyoshi,
H., Chipperfield, M. P., Deushi, M., Dhomse, S. S., Feng, W., Graf, P., Hossaini, R., Jöckel, P., Mancini, E., Michou, M.,
Morgenstern, O., Oman, L. D., Pitari, G., Plummer, D. A., Revell, L. E., Rozanov, E., Saint-Martin, D., Schofield, R., Stenke,
A., Stone, K. A., Visioni, D., Yamashita, Y., and Zeng, G.: Stratospheric injection of brominated very short-lived substances:
370   Aircraft observations in the Western Pacific and representation in global models, J. Geophys. Res.-Atmos., 123, 5690–5719,
https://doi.org/10.1029/2017JD027978, 2018.

Walters, D., Baran, A. J., Boutle, I., Brooks, M., Earnshaw, P., Edwards, J., Furtado, K., Hill, P., Lock, A., Manners, J.,
Morcrette, C., Mulcahy, J., Sanchez, C., Smith, C., Stratton, R., Tennant, W., Tomassini, L., Van Weverberg, K., Vosper, S.,
375   Willett, M., Browse, J., Bushell, A., Carslaw, K., Dalvi, M., Essery, R., Gedney, N., Hardiman, S., Johnson, B., Johnson, C.,
Jones, A., Jones, C., Mann, G., Milton, S., Rumbold, H., Sellar, A., Ujiie, M., Whitall, M., Williams, K., and Zerroukat, M.:
The Met Office Unified Model Global Atmosphere 7.0/7.1 and JULES Global Land 7.0 configurations, Geosci. Model Dev.,
12, 1909–1963, https://doi.org/10.5194/gmd-12-1909-2019, 2019

380   Wargan, K., Orbe, C., Pawson, S., Ziemke, J. R., Oman, L. D., Olsen, M. A., Coy, L., and Emma Knowland, K.: Recent
Decline in Extratropical Lower Stratospheric Ozone Attributed to Circulation Changes, Geophys. Res. Lett., 45, 5166–5176,
https://doi.org/10.1029/2018GL077406, 2018, 2018

Wohltmann, I., P. von der Gathen, R. Lehmann, M. Maturilli, H. Deckelmann, G.L. Manney, J. Davis, D. Tarasick, N. Jepsen,
385   R. Kivi, N. Lyall, and M. Rex, Near complete local reduction of Arctic stratospheric ozone by severe chemical loss in spring
2020, Geophys. Res. Lett., 47, e2020GL089547, doi:10.1029/2020GL089547, 2020.

Zhang, J., Wuebbles, D. J., Kinnison, D. E., & Saiz-Lopez, A.: Revising the ozone depletion potentials metric for short-lived
chemicals such as CF3I and CH3I. Journal of Geophysical Research: Atmospheres, 125, e2020JD032414.
390   https://doi.org/10.1029/2020JD032414, 2020.
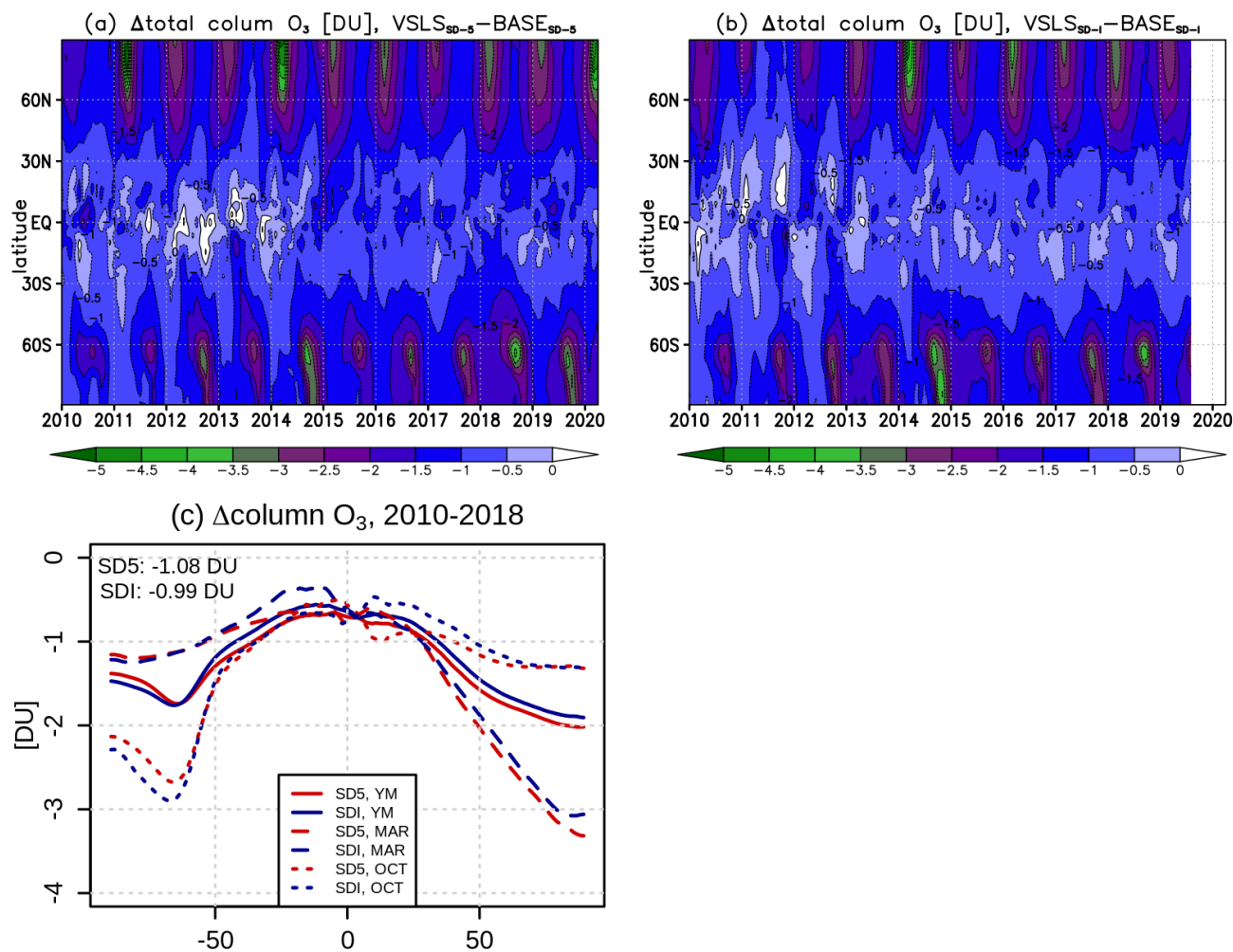
Figure 1. The impacts of Cl-VSLS on recent total column ozone values. Differences in monthly mean total column O_3 as a function of latitude and time (from January 2010 to April 2020) between the pairs of runs with and without Cl-VSLS nudged to either (a) ERA5 ($VSLS_{SD-5}$ and $BASE_{SD-5}$) or (b) ERA-Interim ($VSLS_{SD-I}$ and $BASE_{SD-I}$). Panel (c) shows the yearly mean (solid lines), March (dashed lines) and October (dotted lines) differences averaged over 2010-2018 for runs nudged to ERA5 (red) and ERA-Interim (blue). The values shown in top left corner indicate the respective annual global mean changes over that period.
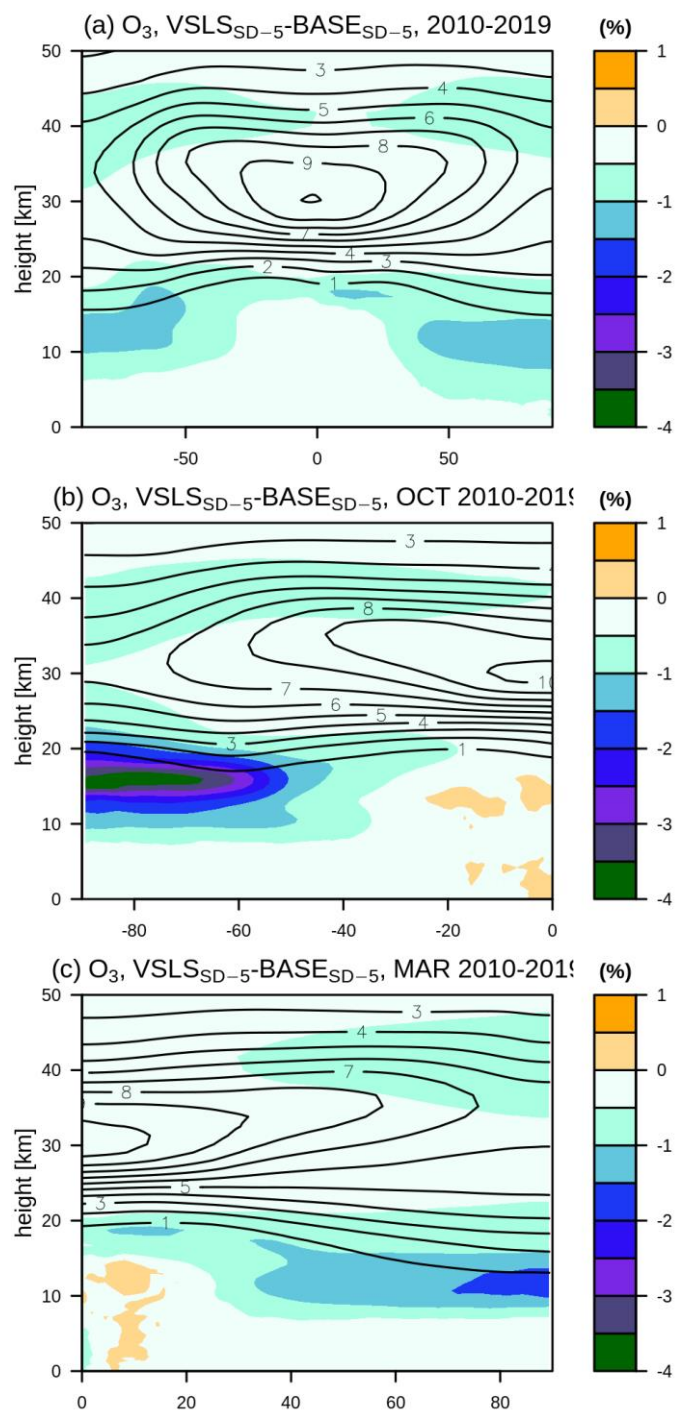
400

Figure 2. The impacts of Cl-VSLS on recent stratospheric ozone levels. Shading: Differences in 2010-2019 (a) yearly mean, (b) October and (c) March ozone [%] between the nudged VSLS_{SD-5} and BASE_{SD-5} runs. Contours show the corresponding ozone values [ppm] in VSLS_{SD-5} for reference.

405
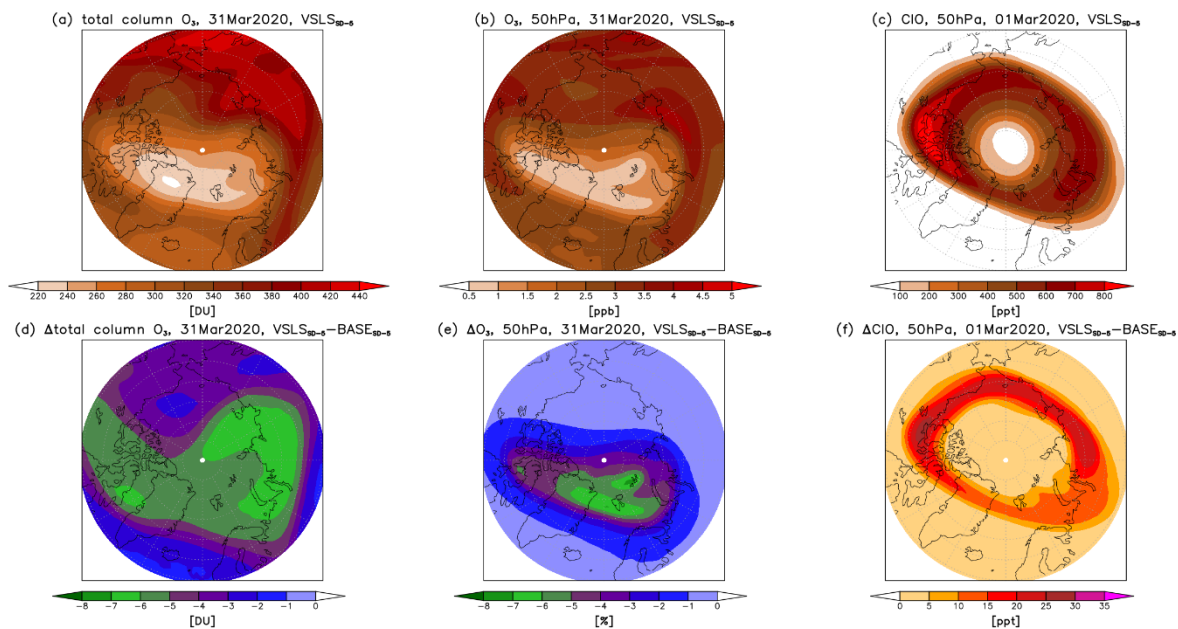
Figure 3. The role of Cl-VSLS during Arctic winter of 2019/2020. Stereographic projections poleward of 60°N of daily mean (a) total column ozone [DU] on 31 March 2020, (b) ozone at 50 hPa [ppb] on 31 March and (c) ClO at 50 hPa [ppt] on 1 March 2020 simulated in the nudged VSLS_SD-5 run. Shown in panels (d-f) are the respective differences between VSLS_SD-5 and BASE_SD-5 runs.

410

Emissions	Δ(TCO3) (±2σ)	Δ(SCO3) (±2σ)
3 Tg- CH_2Cl_2/yr	-3.06 DU (=1.0 %) ±0.80 DU	-2.76 DU ±0.72 DU
0.0350 Tg-CFC11/yr	-3.34 DU (=1.1 %) ±0.76 DU	-3.17 DU ±0.68 DU
CH_2Cl_2 ODP	Total ODP	Stratospheric ODP
	0.0107 (0.0064-0.0175)	0.0102 (0.0062-0.0163)

Table 1. Summary of the terms in the calculation of CH_2Cl_2 ozone depletion potential.

415
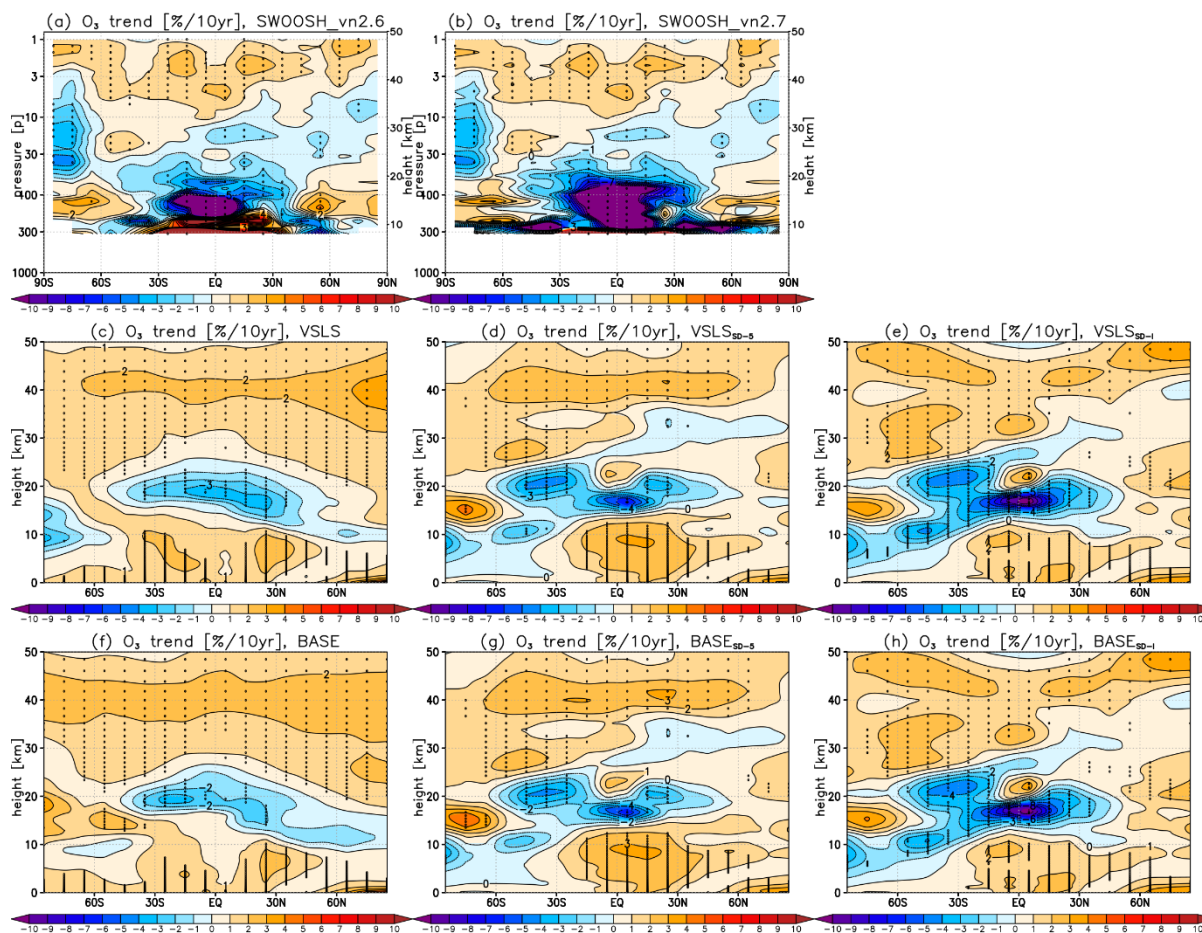
Figure 4. The role of Cl-VSLS in contributing to the recent ozone trends. Linear trends in de-seasonalised O₃ mixing ratios over December 1999 to August 2019 [% per 10 years] in (a-b) the SWOOSH vn2.6 and vn2.7 merged observational product and simulated in (c) the ensemble mean VSLS, (d-e) nudged VSLS_{SD-5} and VSLS_{SD-I}, (f) ensemble mean BASE, and (g-h) the nudged BASE_{SD-5} and BASE_{SD-I}. Hatching indicates statistical significance, here taken as regions where the magnitude of the derived trend exceeds ±2 standard errors.